INSTITUTE OF PHYSICS PUBLISHING PLASMA PHYSICS AND CONTROLLED FUSION

Plasma Phys. Control. Fusion **43** (2001) 1535–1545 PII: S0741-3335(01)25063-5

Density profile measurements by AM reflectometry in TJ-II

T Estrada[1], J Sánchez[1], B van Milligen[1], L Cupido[2], A Silva[2], M E Manso[2] and V Zhuravlev[3]

[1] Laboratorio Nacional de Fusión por Confinamiento Magnético, Asociación Euratom-CIEMAT, 28040 Madrid, Spain
[2] Associação Euratom-IST, CFN, Instituto Superior Técnico, 1096 Lisboa, Portugal
[3] Institute Kurchatov, Institute of Nuclear Fusion, 123182 Moscow, Russia

Received 21 May 2001
Published 18 October 2001
Online at stacks.iop.org/PPCF/43/1535

Abstract

An amplitude modulation reflectometry system is in operation at the stellarator TJ-II. Recently, the first electron density profiles were obtained, showing good agreement with profiles measured by Thomson scattering and lithium beam diagnostics. In order to measure density profiles from the plasma edge, the extraordinary mode of polarization is used. A hyper-abrupt varactor-tuned oscillator used in combination with active multipliers generate two frequency segments: 25–36 and 36–50 etc GHz sharing a unique common wave-guide system (Ka band). The signal is amplitude modulated at 200 MHz and the phase demodulation is done at lower intermediate frequency. The time evolution of the electron density profile was measured under different experimental conditions. In this paper, we present the temporal evolution of the profiles obtained during a transition to an enhanced confinement mode and during cold pulse propagation experiments. We also report the modification in the shape of the density profile measured during a magnetic configuration scan in which a low-order rational surface is moved from the scrape-off layer into the plasma confinement region.

1. Introduction

TJ-II [1] is a flexible helical device with a magnetic field of $B_0 < 1.2$ T, a major radius of 1.5 m and a minor radius of 0.22 m. A notable property of this device is its considerable flexibility with regard to the magnetic configuration. The rotational transform and the magnetic well can be varied over a wide range by changing the current fed into the coil structure consisting of two central coils (circular and helical), two vertical field coils and 32 toroidal field coils. Plasmas are produced and heated by two gyrotrons with frequency $f = 53.2$ GHz and total power $P \cdot 600$ kW (second harmonic, extraordinary mode of polarization).

A high-resolution Thomson scattering diagnostic measures the electron density profile at 160 spatial positions separated by 2.25 mm [2]. Per discharge, a single profile is obtained,

being limited to densities $n_e \cdot 5 \times 10^{12}\,\mathrm{cm}^{-3}$. In addition, the time evolution of the edge and scrape-off layer densities is obtained by means of a lithium beam diagnostic [3]. For the present electron cyclotron resonance heated (ECRH) plasmas, the penetration of the lithium beam allows measurement of densities from the plasma edge to a normalized effective radius of $r_{\mathrm{eff}}/\langle a\rangle \cdot 0.7$. Therefore, in most plasma conditions the density data obtained by both diagnostics do not overlap. The microwave reflectometer installed in TJ-II [4] was designed to cover almost the whole density gradient region of the ECRH plasmas (ECRH cut-off density $n_{\mathrm{cut}} = 1.75 \times 10^{13}\,\mathrm{cm}^{-3}$) with variable time resolution. The reflectometer is an amplitude modulation system, working in the 25–50 GHz range with extraordinary mode polarization.

The microwave reflectometry technique has been applied to the measurement of the electron density profile in fusion devices since the 1980s [5]. The determination of the density profile by microwave reflectometry requires the measurement of the time delay (or differential phase delay) of a probing beam reflected on a plasma with a specific density, the plasma cut-off density. During the 1990s, different techniques were developed to improve the measurement of the time delay, minimizing the perturbations due to plasma turbulence, e.g. fast swept frequency modulated continuous wave (FM-CW), amplitude modulated (AM), two-frequency differential-phase or pulse radar systems. A detailed comparison of the limitations and merits of the different techniques can be found in [6–8].

This paper focuses on the capability of the AM reflectometer to determine the electron density profile in different plasma conditions in TJ-II. The contribution of these measurements to the study of the physical phenomena is also addressed.

The paper is organized as follows. Section 2 is devoted to the description of the main characteristics of the reflectometer. Section 3 outlines the calibration and density profile reconstruction methods and shows a comparison between reflectometry profiles and density profiles obtained using other diagnostics. In section 4, we present experimental results obtained under different scenarios: a transition to an enhanced confinement mode (section 4.1), cold pulse propagation (section 4.2) and a magnetic configuration scan (section 4.3). Finally, some conclusions and future plans are outlined in section 5.

2. System description

A diagram of the reflectometer front end is displayed in figure 1. The system consists of a hyper-abrupt varactor-tuned oscillator (HTO) in the 12–18 GHz range in combination with active multipliers used in alternation. A dual pin switch (SPDT in figure 1) is used to select between the active doubler or tripler paths, i.e. between the two frequency band segments: 25–36 GHz and 36–50 GHz. The oscillator delivers an output power of about 15 dB m. With the multipliers, power outputs of 15–20 dB m are obtained in the complete frequency range. Two separate drivers for the HTO are used, one for each frequency band segment, allowing for an independent adjustment of the minimum and maximum frequencies and therefore permitting some overlapping in the band segments. Both drivers are controlled by a unique tuning signal, while a second control signal is used to select between the two frequency segments. A high-pass filter (FHP: $f \cdot 36$ GHz) is included after the tripler to reduce the second harmonic (it is about 10–20 dB weaker than the third harmonic). The rejection level of the high-pass filter is of 30 dB at $f = 34$ GHz and it is higher at lower frequencies. Therefore the second harmonic signal is at least 40 dB lower than the third one in the whole frequency segment.

The two paths are combined in a Tee hybrid coupler (T). Then, the signal is amplitude modulated using a single pin switch (SW) and a 200 MHz modulation signal.

In the present configuration, the reference signal for the AM system can either be taken from the modulator driver or from a directional coupler installed after the modulator. This

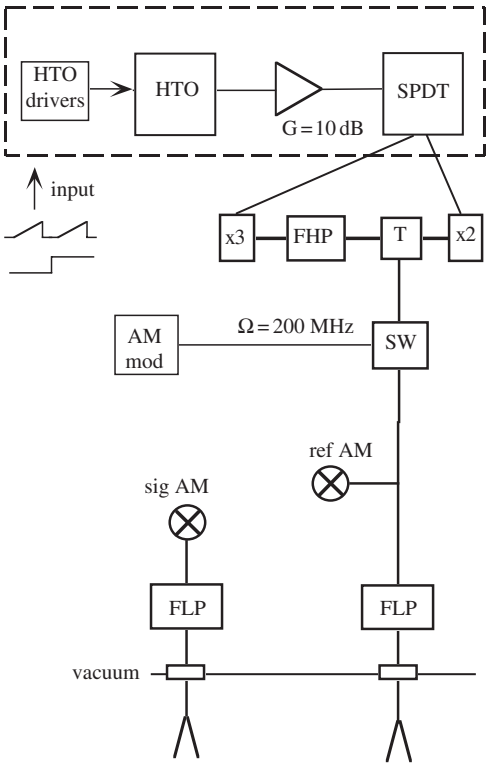

Figure 1. Diagram of the AM reflectometer front end installed in TJ-II.

second possibility avoids the distortion introduced by the phase shift generated at the modulator that may be frequency dependent on the signal frequency. The measurements reported below are obtained exclusively using the signal after the modulator as the reference one.

Low-pass filters (FLP: $f \cdot 50\,\mathrm{GHz}$) have to be included to protect the system against the RF power from the ECRH system. Single-ended mixers are used to obtain the AM envelopes carrying the time delay information. In figure 2, a schematic diagram of the AM receiver is displayed. The phase demodulation of the AM signals is done at a lower intermediate frequency to achieve higher accuracy. The frequency conversion is done using a local oscillator at 189.3 MHz to obtain an intermediate frequency of 10.7 MHz. Then, band pass filters are applied to both the main and the reference signals. The present configuration has filters of 30 kHz bandwidth, though broader filters could also be used in order to increase the time resolution of the profile measurements.

Separate antennas are used for launching and receiving the signal. The antennas are located in the equatorial plane of the toroidal cross-section defined at $\phi = 45^\circ$, and view the plasma from the low-field side. Figure 3 displays the cross-section of the vacuum vessel (it has a diameter of 74 cm) and the arrangement of antennas and in-vessel wave-guides; the last closed magnetic surface for the standard magnetic configuration is also displayed for reference. Inside the vacuum vessel, a fundamental wave-guide is used to transmit the signal from the closest port (A4 top: $\phi = 38.17^\circ, \theta = 90^\circ$) to the desired launching location ($\phi = 45^\circ, \theta = 180^\circ$). The overall insertion losses of all in- and out-vessel components, including the mica plates used as vacuum windows, is about 40 dB.

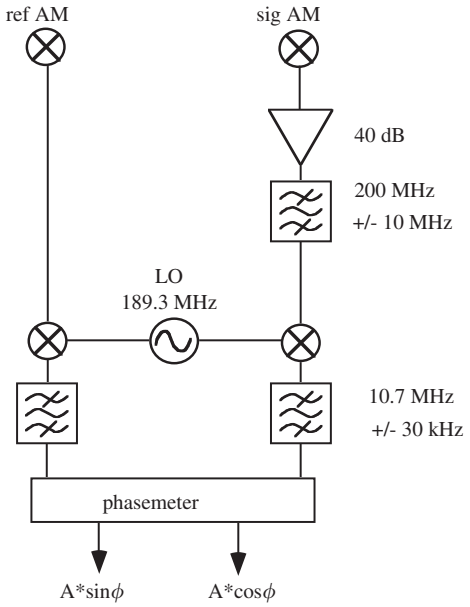

Figure 2. Diagram of the AM receiver.

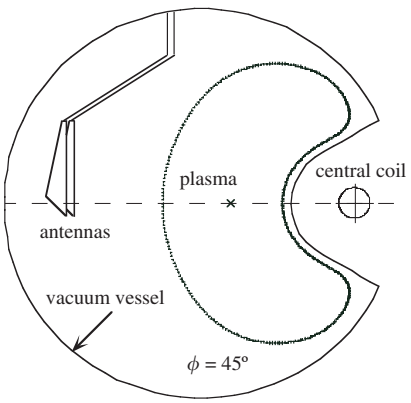

Figure 3. Cross-section of the vacuum vessel and antennas and in-vessel wave-guides arrangement; the last closed magnetic surface for the standard magnetic configuration is also displayed. The broken line represents the equatorial plane of the device.

The launching location was selected since there the magnetic field gradient is parallel to the density gradient. This condition is only satisfied in a small number of locations due to the magnetic field structure of TJ-II, characterized by a strong helical variation of its magnetic axis and a bean-shaped plasma cross-section [1]. Furthermore, at TJ-II, the relative poloidal component of the magnetic field is stronger than what is usual in tokamaks, the angle between the magnetic field lines and the toroidal direction, α, being close to 30° and slightly dependent on the specific magnetic configuration. This dependence is displayed in figure 4 as a function of the upper cut-off frequency, i.e. as a function of the plasma radius, for three specific magnetic configurations. Each magnetic configuration is labelled by the value of the rotational transform at the plasma edge, calculated in vacuum. The support structure of the antennas has been

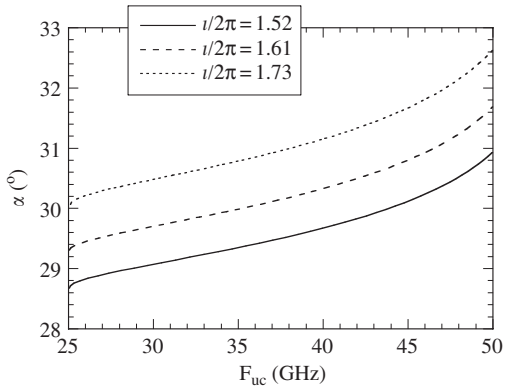

Figure 4. Angle between the magnetic field lines and the toroidal direction as a function of the upper cut-off frequency, i.e. for the different radial locations, in three different magnetic configurations characterized by a rotational transform at the plasma edge equal to 1.52, 1.61 and 1.73, respectively.

designed with an inclination of 30° from the vertical to ensure an almost pure x-mode. An estimation of the error introduced by the variations of α from 30° gives a maximum deviation of the real cut-off frequency with respect to the calculated frequency less than 0.4%. The effects of mode conversion in the beam propagating through the plasma are not significant due to the low magnetic shear of TJ-II.

The reflectometer covers almost the whole density range in all the magnetic configurations during the ECRH phase of TJ-II ($B = 1$ T, $f_{\mathrm{ECRH}} = 53.2$ GHz, $n_{\mathrm{cut}} = 1.75 \times 10^{13}$ cm^{-3}). The highest reflecting density at the magnetic axis (for the maximum incident frequency: 50 GHz) is close to 1.4×10^{13} cm^{-3} for most of the magnetic configurations of TJ-II. Nevertheless, due to the flat density profiles, characteristic of TJ-II [9], central densities are not accessible even for low plasma density discharges. The lowest reflecting densities at the plasma edge (incident frequency: 25 GHz) range from 0 to 3×10^{11} cm^{-3}. These low cut-off densities, together with the fact that the magnetic field at the plasma edge is more accurately known in stellarators than in tokamaks, alleviate the initialization problem.

For NBI heating plasmas with higher electron densities, additional frequency channels will be needed.

3. Calibration procedure

In most reflectometry systems, the time delay of the microwave beam inside the plasma is much smaller than the time delay due to propagation through the wave-guides and through vacuum. Therefore it is indispensable to perform a calibration of the time delay of the beam outside the plasma, taking a fixed reference. A standard procedure for the calibration consists of measuring the time delay of the signal reflected on the inner vessel wall. In TJ-II, this signal is very weak because of the shape of the inner wall. The vacuum chamber cross-section is not circular, and it has a groove (at the position of the central coil) just in front of the antennas (see figure 3). Thus, the inner vessel wall is not a concave but a convex surface. Nevertheless, the time delay of the signal reflected in the inner vessel wall can be measured with the AM reflectometer except for the higher frequencies. At $f > 43$ GHz, the amplitude of the signal is too low and the time delay cannot be measured accurately. Therefore it is possible to calibrate the system for any change in the microwave transmission line in the frequency range from 25

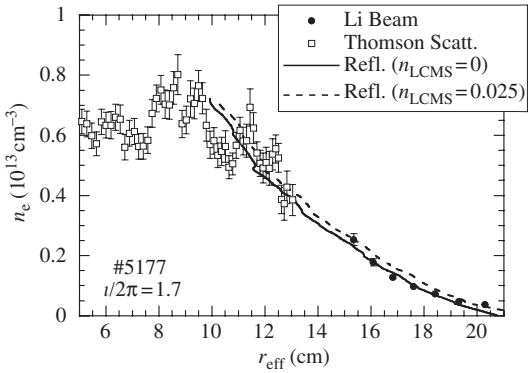

Figure 5. Electron density profiles measured with three diagnostics: Thomson scattering system (□), lithium beam diagnostic (●) and AM reflectometer, in a plasma with low density, injected power $P_{ECH} = 300$ kW and magnetic configuration with edge rotational transform of 1.70. The reflectometry profiles are obtained considering two different values of the density at LCMS: equal to zero (——) and equal to the density measured by the Li beam diagnostic (- - - -).

to 43 GHz during the experimental campaign. This range limits the maximum probed density to $n_{max} \cdot 0.8 \times 10^{13}$ cm^{-3} for the typical magnetic field of TJ-II.

The reconstruction of the density profile from the measured time delay is done using the Bottollier algorithm [5]. At TJ-II, the position of the last closed magnetic surface and the magnetic field profile depend on the magnetic configuration. To reconstruct the density profile, we choose the theoretical position of the last closed magnetic surface as the starting point for the initialization of the profile ($n_{LCMS} = 0$) and use a linear density ramp up to the first reflecting point (close to $n_{ini} = 3$–4×10^{11} cm^{-3}). The condition of continuous density gradient at the first probed density is imposed to determine the slope of this initial profile.

The density profiles obtained by reflectometry were compared with the profiles obtained by the high-resolution Thomson scattering system [2] and by the lithium beam diagnostic [3]. Taking into account that the radial range covered by the reflectometer only overlaps with that of the Thomson scattering and the lithium beam diagnostic for small sections, the agreement is in general very good. As an example, the profiles measured with the three diagnostics are shown in figure 5, for a plasma with low density, in a magnetic configuration with $\iota/2\pi = 1.7$ and with heating power $P_{ECH} = 300$ kW. The spread in the Thomson scattering data is due to the presence of 'structures' in the electron density profile. In [10] the characteristics of these structures are described and their possible origin is discussed. The discrepancy between the density profiles at the most internal radial locations ($r_{eff} \cdot 10$ cm in figure 5) could be explained in terms of the impossibility of measuring negative density gradients with the reflectometer.

The assumption of zero density at the last closed magnetic surface may introduce an error in both the shape of the density profile and the absolute position of the density profile within the vacuum vessel. In figure 5 the density profile obtained for a density value at LCMS equal to the one measured by the Li beam diagnostic ($n_e = 0.025 \times 10^{13}$ cm^{-3}) is also displayed (broken line). We observe that the uncertainty in the absolute plasma position is about half a centimetre. However, the density gradient is almost insensitive to the position of the plasma edge, allowing the study of the evolution of the density profile shape without additional information from other diagnostics.

In the reconstruction of all the density profiles reported below, we have considered the last closed magnetic surface as the starting point for the profile initialization.

4. Experimental results

The time evolution of the density profile was measured under different experimental conditions. In this paper we present some results obtained during a transition to an enhanced confinement mode and during cold pulse propagation experiments. The time resolution of these measurements is 2 ms. The change in the shape of the density profile obtained during a magnetic configuration scan in which the low-order rational surface of $\iota/2\pi = 4/2$ is moved from the scrape-off layer into the plasma confinement region is described.

4.1. Transition to an enhanced confinement mode

Under some experimental conditions, a transition to an enhanced confinement mode is obtained. First experimental observations have been reported recently in [11]. In this type of discharges, the average density measured by the microwave interferometer increases continuously after the transition even when the external puffing rate decreases. As explained in [11], the particle confinement time increases by a factor of three. The rise in the central electron density is also confirmed by the Thomson scattering system, measuring on a shot to shot basis.

The time evolution of the density profiles was measured recently during this transition using the AM reflectometer. In figure 6(*a*), the average density measured by the microwave

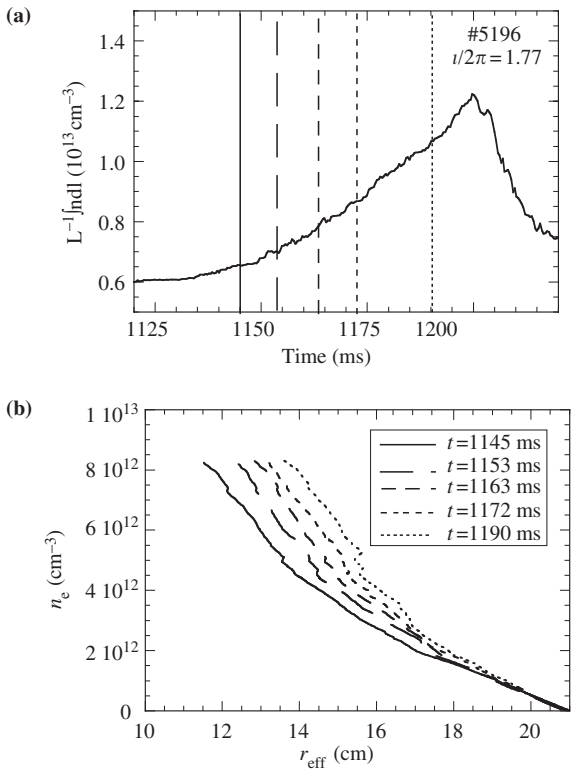

Figure 6. Time evolution of the averaged electron density measured by the microwave interferometer (*a*) and density profiles measured by the reflectometer (*b*) during the transition to an enhanced confinement mode. Each vertical line in (*a*) represents the time at which the corresponding density profile is measured.

interferometer is displayed. After the transition ($t \cdot 1150$ ms), the line average density increases continuously, reaching the ECH cut-off density at $t \cdot 1200$ ms. Figure 6(*b*) shows the evolution of the density profile measured by reflectometry. The time at which each profile is evaluated is marked by a vertical line in figure 6(*a*).

Two different regions can be distinguished in the density profiles. In the most external part (from $r_{\mathrm{eff}} \cdot 18$ cm to the last closed magnetic surface located at $\langle a \rangle = 21$ cm), the density profile remains almost constant, and only a slight increase in the density is observed. However, a noticeable change in the density profile is observed in the region $r_{\mathrm{eff}} < 18$ cm where a continuous increase in the density gradient and a broadening of the profile takes place. The rate at which the profile broadens is high just after the transition and decreases afterwards. Assuming a flat density profile in the plasma centre and taking into account the average density measured by the interferometer, the time evolution of the whole density profile can be evaluated. Just after the transition, the profile broadens while the central density remains almost constant. However, thereafter the broadening is less pronounced and the density at the plasma centre increases reaching the ECRH cut-off value.

The possible correspondences between this transition and the transition to H-modes observed in many devices are being evaluated and will be reported in a separate paper.

4.2. Cold pulse propagation experiments

Recently, nitrogen pulses have been injected in the scrape-off layer of TJ-II to study impurity transport and radiation behaviour. To illustrate the response of the density profile to the injected pulse, we have chosen a discharge in which the amount of nitrogen is rather large. The average electron density, as measured by the microwave interferometer, increases by nearly 15%. Reflectometry measurements show an increase in the density when the nitrogen pulse is injected. Three density profiles obtained just before the pulse and 2 and 6 ms later are displayed in figure 7. In this magnetic configuration, the last closed magnetic surface is located at $\langle a \rangle = 20$ cm. Two milliseconds after the pulse, the most pronounced increase in the density is measured in the range $r_{\mathrm{eff}} = 12$–16 cm, and in the next milliseconds the perturbation in the density propagates to more internal radial locations. The time evolution of the perturbation in the density profile is shown in figure 8 as a contour plot of constant density lines. Within the time resolution of 2 ms, the perturbation occurs simultaneously in the most external radial locations ($r_{\mathrm{eff}}/\langle a \rangle \cdot 0.7$). Further inside, it is possible to measure the inward propagation of the pulse

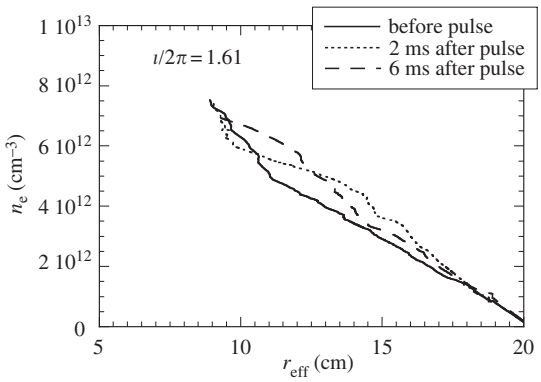

Figure 7. Modification in the density profile due to a nitrogen pulse injected in the scrape-off layer of TJ-II. Three profiles are shown: just before the pulse and 2 and 6 ms later.

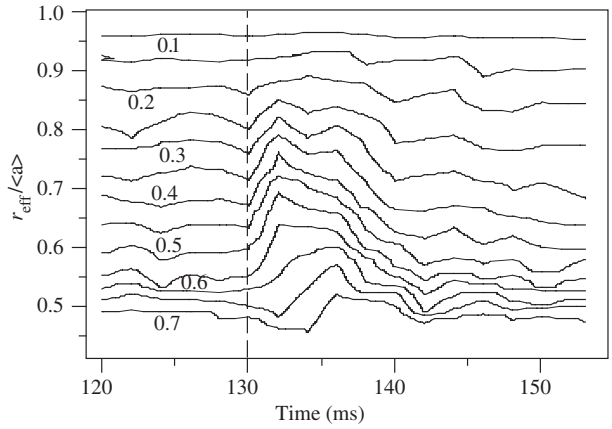

Figure 8. Contour plot of the constant density lines showing time evolution of the perturbation in the density profile. The vertical line indicates the time at which the pulse is injected.

and therefore the particle diffusion coefficient. From the data shown in figure 8 one obtains a particle diffusion coefficient of $D \cdot 0.1\ \mathrm{m^2\ s^{-1}}$ at $r_{\mathrm{eff}}/\langle a\rangle = 0.5$–$0.7$. This value is comparable to the neoclassical particle diffusion coefficient calculated using the monoenergetic Monte Carlo technique [12]. The diffusion coefficient calculated for these particular experimental conditions ranges from $D \cdot 0.15\ \mathrm{m^2\ s^{-1}}$ at the plasma centre to $D \cdot 0.1\ \mathrm{m^2\ s^{-1}}$ at $r_{\mathrm{eff}}/\langle a\rangle = 0.4$. On the other hand, if we apply for TJ-II the parameter dependence of the diffusion coefficient that has been obtained in W7-AS stellarator from perturbative particle transport studies [13], a coefficient of $D \cdot$ 0.3–0.4 $\mathrm{m^2\ s^{-1}}$ is obtained. Due to the large experimental error in the determination of the diffusion coefficient, mainly caused by the low temporal resolution of the density profile measurements, we consider the obtained value to be roughly consistent with both predictions.

The evolution of the electron density profile measured by the AM reflectometer during these experiments is an important element in the study of the transport properties of the plasma. Indeed the measurements presented here provide the first experimental estimates of the particle diffusion coefficient at the plasma interior of TJ-II. More detailed analyses of radiation evolution and transport are underway.

4.3. Low-order rational surfaces

The flexibility and low magnetic shear of TJ-II allows a very precise control of the rotational transform profile and its rationals [14]. Reflectometry measurements have been obtained during a magnetic configuration scan. In this scan, the rational surface $\iota/2\pi = 4/2$ was moved from the scrape-off layer into the plasma confinement region.

Due to the four-fold periodicity of TJ-II, the presence of a rational surface of fourth order, $\iota/2\pi = (n = 4)/\mathrm{m}$, in the magnetic configuration leads to the appearance of magnetic islands called 'natural' islands [14]. In these magnetic configurations the definition of the averaged radius for each magnetic surface is not valid anymore. Therefore the density profiles obtained in this experiment are represented as a function of the plasma major radius which coincides with the reflectometer line of sight (see figure 3).

The appearance of this low-order rational surface inside the plasma is observed as a local flattening of the electron density profile measured using the reflectometer. Figure 9(*a*)

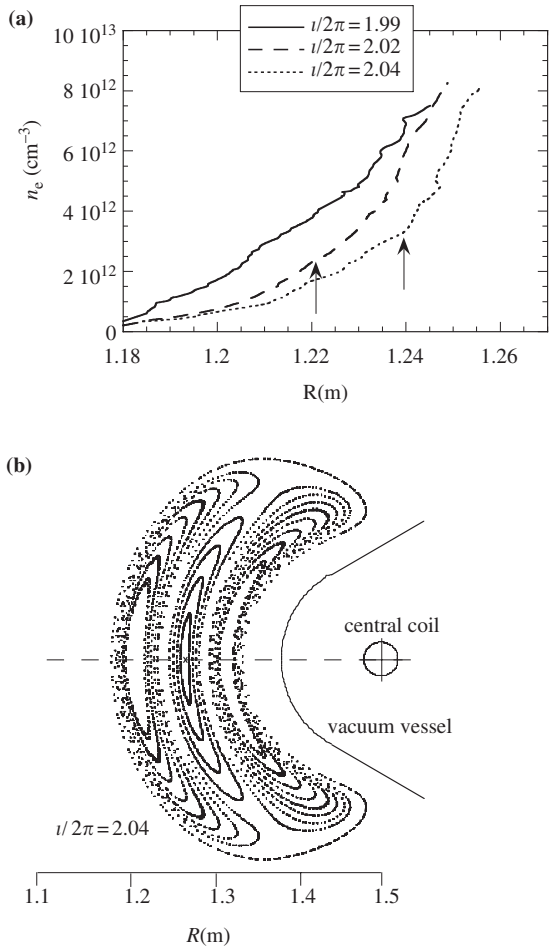

Figure 9. (*a*) Density profiles obtained in a magnetic configuration scan in which the rational surface $\iota = 4/2$ moves from the scrape-off layer (configuration with $\iota/2\pi = 1.99$) into the plasma confinement region (configurations with $\iota/2\pi = 2.02$ and 2.04). The island ranges from the plasma edge to the radial positions marked with arrows. (*b*) Flux surfaces computed by equilibrium codes for the configuration with an edge rotational transform of 2.04.

displays the density profiles obtained in three magnetic configurations. The plasma centre in these magnetic configurations is located at $R = 1.27$ m. The rational surface $4/2$ is just outside the last closed magnetic surface in the magnetic configuration with $\iota/2\pi = 1.99$. Decreasing the current in the circular coil and increasing that of the helical coil, the rotational transform increases and the rational surface moves into the plasma. The flux surfaces computed by the equilibrium codes in the configuration with $\iota/2\pi = 2.04$ are displayed in figure 9(*b*). The width of the island in this configuration is almost as large as the main plasma. The island width computed with equilibrium codes increases from $w \cdot 0.04$ m in the configuration with $\iota/2\pi = 2.02$ to $w \cdot 0.06$ m in the configuration with $\iota/2\pi = 2.04$ (figure 9(*b*)). It spreads from the plasma edge to the positions marked with arrows in figure 9(*a*). We observe that the radial range of the flattening in the density profile increases as the radial extent of the magnetic island predicted theoretically does.

5. Conclusions and future plans

First electron density profiles have been obtained in TJ-II using AM reflectometry. The comparison between reflectometry profiles and profiles measured using other diagnostics shows a good agreement. Hence, no strong influence of plasma turbulence on the profile measurement has been detected. The experimental results presented in this paper have shown the importance of this kind of measurement. However, in its present configuration, the time resolution of the system is not sufficiently high, specifically for measurements during pulse propagation experiments. In order to obtain density profiles with high time resolution, broader filters will be used as the last filters of the AM receiver. In addition, the reflectometer will be modified to operate simultaneously in the AM and FM-CW modes, with frequency sweep times as fast as 40 μs for the whole frequency range.

Acknowledgments

The authors wish to thank the members of the TJ-II team, particularly I Pastor and J Herranz for the Thomson scattering data, B Brañas, D Tafalla and F L Tabarés for the lithium beam data, V Tribaldos for the neoclassical transport calculations and A López-Fraguas for the equilibrium calculations.

References

[1] Alejaldre C *et al* 1999 *Plasma Phys. Control. Fusion* **41** A539
[2] Barth C J, Pijper F J, Meiden H J v d, Herranz J and Pastor I 1999 *Rev. Sci. Instrum.* **70** 763
[3] Brañas B, Tafalla D, Tabarés F L and Ortiz P 2001 *Rev. Sci. Instrum.* **72** 602
[4] Estrada T, Cupido L, Meneses L, Sánchez J and Manso M E 1999 *Proc. IV Technical Committee Meeting on Microwave Reflectometry for Fusion Plasma Diagnostics (Cadarache)* EUR-CEA-FC-1674
[5] Bottolier H and Ichtchenko G 1987 *Rev. Sci. Instrum.* **58** 539
[6] Doyle E J, Kim K W, Lee J H, Peebles W A, Rettig C L, Rhodes T L and Snider R T 1996 *Diagnostics for Experimental Thermonuclear Fusion Reactors*, ed P E Stott, G Gorini and E Sindoni (New York: Plenum) p 117
[7] Laviron C, Donné A J H, Manso M E and Sánchez J 1996 *Plasma Phys. Control. Fusion* **38** 905
[8] Mazzucato E 1998 *Rev. Sci. Instrum.* **69** 2201
[9] Alejaldre C *et al* 1999 *Plasma Phys. Control. Fusion* **41** B109
[10] Herranz J, Pastor I, Castejón F, de la Luna E, García-Cortes I, Barth C J, Ascasíbar E, Sanchéz J and Tribaldos V 2000 *Phys. Rev. Lett.* **85** 4715
[11] Tabarés F L, Brañas B, García-Cortés I, Tafalla D, Estrada T and Tribaldos V 2001 *Plasma Phys. Control. Fusion* **43** 1023
[12] Tribaldos V 2001 *Phys. Plasmas* **8** 1229
[13] Koponen J P T, Geist T, Stroth U, Fiedler S, Hartfuss H J, Heinrich O, Walter H and Dumbrajs O 2000 *Nucl. Fusion* **40** 365
[14] Ascasíbar E, Qin J and López-Fraguas A 1998 *J. Plasma Fusion Res. Series* **1** 183